

BEHM-GAN: Bandwidth Extension of Historical Music using Generative Adversarial Networks

Eloi Moliner and Vesa Välimäki, *Fellow, IEEE*

Abstract—Audio bandwidth extension aims to expand the spectrum of narrow-band audio signals. Although this topic has been broadly studied during recent years, the particular problem of extending the bandwidth of historical music recordings remains an open challenge. This paper proposes BEHM-GAN, a model based on generative adversarial networks, as a practical solution to this problem. The proposed method works with the complex spectrogram representation of audio and, thanks to a dedicated regularization strategy, can effectively extend the bandwidth of out-of-distribution real historical recordings. The BEHM-GAN is designed to be applied as a second step after denoising the recording to suppress any additive disturbances, such as clicks and background noise. We train and evaluate the method using solo piano classical music. The proposed method outperforms the compared baselines in both objective and subjective experiments. The results of a formal blind listening test show that BEHM-GAN significantly increases the perceptual sound quality in early-20th-century gramophone recordings. For several items, there is a substantial improvement in the mean opinion score after enhancing historical recordings with the proposed bandwidth-extension algorithm. This study represents a relevant step toward data-driven music restoration in real-world scenarios.

Index Terms—Audio recording, machine learning, music, signal restoration, convolutional neural networks.

I. INTRODUCTION

HISTORICAL music recordings are available in large numbers in archives but, due to the technological limitations of the time, by modern standard they are of a very poor audio quality. Early-20th-century gramophone recordings suffer from severe degradations, such as multiple kinds of surface noises, distortion, and a narrow frequency bandwidth [1], [2]. The goal of digital audio restoration is to correct the imperfections of audio recordings so that the resulting sound quality is enhanced. Restoration may target the removal of clicks and noises [3], [4], the inpainting of missing audio segments [5], [6], declipping [7], or the bandwidth extension of narrow-band audio signals, among other tasks.

This paper focuses on audio bandwidth extension and, particularly, on applying it to historical music recordings. During recent years, many works have used modern deep learning technologies for bandwidth extension, but usually with the final goal of increasing the sampling rate of modern digital audio signals. Only a few exceptions are relevant to music signal processing [8], [9], [10], whereas most of these studies focus on processing speech [11], [12], [13], [14], [15].

Manuscript received February 16, 2022. This research is part of the activities of the Nordic Sound and Music Computing Network—NordicSMC, NordForsk project no. 86892. (Corresponding author: Eloi Moliner)

E. Moliner and V. Välimäki are with the Acoustics Laboratory, Department of Signal Processing and Acoustics, Aalto University, Espoo, Finland (e-mail: eloi.moliner@aalto.fi).

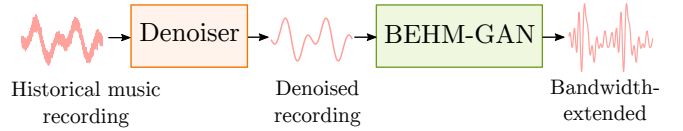


Fig. 1. Illustration of the inference pipeline. The denoiser block refers to a model borrowed from earlier work [17], and the BEHM-GAN is the model proposed in this paper.

Although music and speech share the same domain of acoustic signals, both of these signals are fundamentally different.

Usually, the aforementioned methods are trained in a self-supervised fashion by pre-processing the audio data with lowpass filters to simulate the bandwidth limitation. Then, the models are optimized to extend the input lowpass-filtered audio using the broadband original signal as a target. However, bandwidth-extending historical recordings entails an extra challenge, as no full-bandwidth version is available for this particular material. Then, we would rely on the model, trained with synthetically filtered data, to extrapolate to real historical recordings, a harder out-of-distribution scenario. One should also consider the problem of filter generalization [16], which refers to the inability deep neural networks to generalize when they are trained using a single type of lowpass filter in the training-data pipeline.

Another problem with old gramophone recordings is that they are often corrupted with a wide range of global and local disturbances, such as hiss, clicks, and thumps. These additive noises represent another obstacle in enhancing the recording. Luckily, recent works have shown that a vast majority of clicks and noises appearing on gramophone recordings can be efficiently suppressed using deep-learning models [4], [17]. We studied this problem in particular and proposed a model consisting of a complex-spectrogram-based deep-neural-network architecture [17]. The denoising model was trained using a realistic dataset of noise samples extracted from gramophone recordings and yields a considerable enhancement in quality [17]. This paper builds upon this previous work [17], in such a way that the proposed bandwidth extension method is intended to be applied as a second step after the original recording has been first denoised, as illustrated in Fig. 1.

In this paper, we present BEHM-GAN, a bandwidth-extension method that can be effectively applied to historical music recordings. The proposed method is based on a generative adversarial network (GAN) [18] and combines a generator in the complex-spectrogram domain with multiple time-domain discriminators. To provide the model with the necessary robustness to make inference in historical recordings, we propose a simple but effective filter regularization in

the training stage. The strategy is based on adding a small amount of white Gaussian noise after applying a lowpass filter with a randomized cutoff frequency. We show that the proposed method inserts sound energy in an appropriate way above the cutoff frequency of about 3 kHz and, as determined in a formal blind listening test, significantly improves the perceived quality of both artificially bandlimited and real old piano music. As far as we are aware, this is the first work that successfully extends the bandwidth in real historical music recordings. We emphasize that the goal of this work is not to restore exactly the missing sound events, but to recreate plausible high-frequency content and, thus, make the music more pleasant to listen to.

The remainder of this paper is organized as follows. Sec. II reviews the most relevant related work, with a focus on recent deep-learning-based audio-bandwidth-extension studies. To understand the bandwidth limitation of historical gramophone recordings, Sec. III analyzes empirically their spectral characteristics using the long-term average spectrum (LTAS). The proposed BEHM-GAN method is introduced in Sec. IV and is evaluated in Sec. V with objective and subjective metrics. In order to assess the robustness of the compared methods, the experiments are conducted under two separate conditions: lowpass filtered modern recordings and old historical recordings. Finally, Sec. VI concludes the paper.

II. RELATED WORK

This section reviews previous work on audio bandwidth extension, focusing on approaches that apply GANs for related tasks or study the problem of filter generalization.

A. Audio Bandwidth Extension

Audio bandwidth extension refers to methods that extend the spectrum of audio signals [19]. A popular sub-topic is audio super-resolution [11], [12], which increases the sampling rate of a given audio signal by extending its bandwidth above the original Nyquist limit. This topic has a long history in telephony, where the bandwidth of a transmitted speech signal was usually compressed because of channel constraints [20]. Another relevant application is audio compression, as bandwidth-extension techniques can be used to reduce the bit rate of an audio signal [21], [22].

Early works used signal processing methods such as a source-filter model [23], nonlinear devices [19], or spectral band replication [24]. Other approaches were based on data-driven techniques, such as Gaussian mixture models [25], [26], hidden Markov models [27], or shallow neural networks [28], [29]. However, due to their inadequate modeling capabilities, these early methods often lead to a poor or mediocre audio quality.

More recently, deep-learning-based bandwidth extension-methods outperformed previous approaches. The vast majority of the presented methods used convolutional neural networks and work using either a spectrogram representation [30], [31], raw audio data [11], [32], [33], [12], or a mixture of both [34], [35].

B. GANs for Audio Bandwidth Extension

Deep learning models based on optimizing reconstruction losses excel at tasks where the goal is to design a nonlinear mapping between two data distributions, e.g., denoising. However, the performance of supervised learning is limited when the task involves generating new content that is absent in the observed signal, as is the case in bandwidth extension. As a consequence, deep learning tends to build over-smoothed and unrealistic spectra. For this reason, recent works have adopted a generative approach that allows the model to have more expressive power. Some studies applied different kinds of generative models for the task of speech bandwidth extension, such as flow-based models [36] or diffusion-probabilistic models [15], but, in particular, GANs [18] have shown great potential for this task.

GANs are generative models that are based on optimizing a two-player min-max game between a generator G and a discriminator D [18]. The discriminator D is optimized to distinguish real data samples from the ones generated by G , whereas G tries to fool D by generating data samples that are harder to detect. Ideally, if the training does not collapse, both G and D will converge to the so-called Nash equilibrium, where G fits the target data distribution and D is unable to detect the fake data samples from the real ones. In the original GAN formulation, a latent vector of Gaussian noise z is provided to the generator $G(z)$ as an input. However, GANs for audio bandwidth extension can be viewed as conditional GANs [37], where the generator $G(x, z)$ is also conditioned on an observed signal x , here the narrow-band input. Then, due to the high dimensionality of x , the latent vector z is often omitted if a controllable latent-space representation is not required [38].

Although only a few studies have applied GAN models to bandwidth extension of music signals [10], [39], many recent works have applied them for speech [14], [13], [40]. Eskimez *et al.* [40] proposed one of the earliest works using an adversarial approach for speech super-resolution. Their proposed model predicted the magnitude spectrogram representation of audio and used an adversarial loss combined with a reconstruction loss. However, the Eskimez model had the limitation that it did not predict the phase information but just replicated it [40]. Other phase-aware works made an effort to incorporate the phase information into the training framework [10]. Instead, Kim *et al.* [39], opted for working directly on raw audio, thus avoiding the aforementioned phase issues. They also incorporated a third auxiliary feature-matching loss term. Su *et al.* [13] used a time-domain Wavenet generator and a composite of multiple time-domain and spectral-domain discriminators. Utilizing a complex combination of loss terms, they achieved impressive results. Li *et al.* [14] proposed a lighter time-domain model that was suitable to run in real-time.

C. Lowpass Filter Generalization

A particular problem in the audio-bandwidth-extension literature is the incapability of deep neural networks to generalize when they are trained using lowpass filters. We hypothesize

that this problem is a special case of shortcut learning [41], stating that the model does not learn the true underlying mechanisms of the data but relies on spurious statistical relationships. In this case, the neural network learns the easier task of inverting the response of a lowpass filter instead of generating new and coherent high-frequency content.

Kuleshov *et al.* [11] observed that a neural network trained to conduct audio super-resolution using aliased training data was ineffective if an antialiasing filter was included during testing. The same problem happened when antialiasing filters were only used during training and when the filters utilized during training and testing differed. Sulun and Davies [16] studied this phenomenon and named it "filter overfitting". They showed that the problem could be mitigated considerably by using a set of different lowpass filters during training as a data augmentation strategy.

Wang and Wang [12] examined the robustness of their speech super-resolution model that was trained with different down-sampling schemes. They proposed a solution based on randomly combining three different down-sampling strategies during training. Li *et al.* [14] also experimented with using variable-band filters with randomized cutoff frequencies to increase the robustness of the model in real-life speech bandwidth-extension scenarios. Similarly, Nguyen *et al.* [42] applied anti-aliasing filters having random order and ripple intending to improve the robustness of their model.

This problem gets more relevant in the case of historical recordings when we aim to infer a target distribution that has not been processed by any lowpass filter. In this case, neither a specific filter specification nor a known cutoff frequency can be assumed, since they may vary greatly depending on the recording conditions. In the next section, we investigate the underlying lowpass filtering in old gramophone recordings.

III. SPECTRAL ANALYSIS OF GRAMOPHONE RECORDINGS

To obtain prior knowledge to design our method, we analyzed the bandwidth of 78-RPM (rounds per minute) gramophone recordings, which we were interested in enhancing. To fully understand the frequency characteristics of these recordings, one must study the recording conditions of the time. However, due to the lack of international standards, the exact characteristics vary widely depending on the manufacturer, the publication date, the recording material, or possible equalization corrections made by recording engineers. Hence, the work of audio restoration is extremely hard, as restoration engineers now have to conduct a study on industrial archaeology for every single record they aim to restore [43].

One of the main reasons for the limited bandwidth in old analog recordings are the disc-cutting lathes, used to record sound into the physical disc media [43]. The most critical piece, the cutterhead, converts electric waveforms into modulations in a groove. The frequency response of the recording vary greatly depending on the cutterhead model, the speed of the record, or the shape of the stylus. The most commonly used cutterheads during the 1920s and 1930s produced a resonance frequency between 3 kHz and 4 kHz, and above that the frequency response decayed rapidly. As a consequence, due

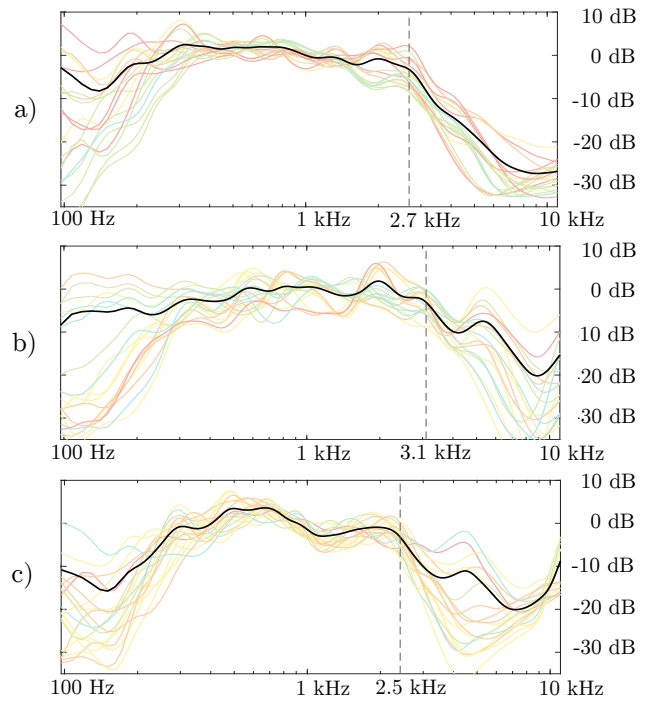


Fig. 2. LTAS difference curves computed between six pre-1930s recordings and three contemporary recordings of (a) *The Blue Danube Waltz*, (b) *Carmen*, and (c) *Humoresque*. Each colored line represents the difference between the LTAS of one of the six old recordings and one of the three modern ones, totalling 18 curves. The black line is the average of the difference curves, and the vertical dashed line marks its -3 -dB point.

to the poor signal-to-noise ratio (SNR) of the recordings, the high-frequency components above this resonance frequency were practically lost. Over the years, better equipment was developed that allowed engineers to extend the recordable bandwidth of audio, thanks to many technological advances like motional feedback [43].

To analyze empirically the spectral characteristics of 78-RPM gramophone recordings, we conduct a study based on the LTAS. To do so, we collected six 78-RPM gramophone recordings of a given music piece, all of them containing a similar ensemble of instruments and dated before the year 1930. For comparison, we also collected three contemporary broadband recordings of the same piece. The six old recordings were first denoised using our previously proposed method [17]. The LTAS was calculated for each of the recordings using the IoSR library [44], applying Gaussian smoothing per octave band. We then subtract the LTAS of the three contemporary recordings from each of the old versions to obtain a rough estimate of the frequency response of the recording. The resulting 18 difference LTAS curves are re-scaled so that their mean level between 500 Hz and 2 kHz is 0 dB.

Fig. 2 shows the computed difference LTAS curves and their average for three classical pieces: the orchestral piece *The Blue Danube Waltz*, by Johann Strauss (Fig. 2(a)); the opera piece *L'amour est un oiseau rebelle*, from *Carmen* by Georges Bizet (Fig. 2(b)); and *Humoresque No. 7*, by Antonin Dvořák, played by string ensembles (Fig. 2(c)). Although these plots do not give accurate information due to the averaging and the octave-band smoothing, they indicate a decaying trend

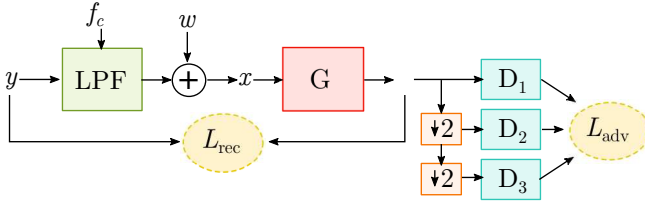


Fig. 3. Proposed GAN-based training framework containing generator G , three time-domain discriminators D_1 , D_2 , and D_3 , a variable lowpass filter (LPF), and additive noise w . The training is optimized with a composite of two losses: an adversarial loss L_{adv} and a reconstruction loss L_{rec} .

starting at approximately 3 kHz. The estimated -3 -dB cutoff frequencies are 2.7, 3.1, and 2.5 kHz for the above-mentioned historical recordings, as indicated in Fig. 2.

IV. BEHM-GAN

This section presents the BEHM-GAN, the proposed method for the bandwidth extension of historical recordings. The BEHM-GAN is a GAN-based model that is trained in a self-supervised manner by using lowpass filters to simulate the lack of high-frequency content in old recordings. The training framework is summarized in Fig. 3.

A. Generator Model Architecture

We opt to work in the complex-spectrogram domain to design our generator. Thus, the input narrow-band audio x sampled at $f_s = 22.05$ kHz is first transformed by means of the short-time fourier transform (STFT). We use an FFT length of 1024 samples (46 ms) with a Hamming window of the same size and a hop length of 256 samples (12 ms). The resulting complex signal is converted to real one by stacking its real and imaginary parts as separate channels. Then, assuming that the generator succeeds at maintaining the implicit phase information, the output signal can be directly converted back to the time domain using the inverse-STFT, without the need of a phase-recovery technique.

The generator architecture is based on the U-Net model [17] and is shown in Fig. 4. The architecture is formed by 2D-convolutions and Exponential Linear Unit non-linearities [45] to capture time-frequency features from the complex spectrogram. We concatenate frequency-positional embeddings [46] as an inductive bias to break the frequency-equivariance symmetry, which is implicit in 2D-convolutions. The architecture has an encoder-decoder structure with residual DenseNet blocks [47] as intermediate layers. The encoder coarsens the resolution at each layer using strided convolutions, sequentially increasing the number of channels. The decoder structure is symmetrical to the encoder and upsamples the resolution with transposed convolutions. The concatenative skip connections help to retain fine-grained details of the spectrogram. We refer the reader to the source code¹ for further details on the model implementation and the used hyperparameters.

B. Training Objective

The generator is optimized with a composite of two losses, an adversarial loss L_{adv} and an auxiliary reconstruction loss L_{rec} :

$$L_G = L_{\text{adv}} + \alpha L_{\text{rec}}, \quad (1)$$

where the coefficient $\alpha = 0.4$ is a tuning hyperparameter used to combine the two loss terms. For the adversarial loss, we adopt the multi-scale discriminators D_1 , D_2 , and D_3 from MelGAN [48].

As indicated in Fig. 3, discriminator D_1 operates directly on the raw audio waveform, whereas the input waveforms of discriminators D_2 and D_3 are, respectively, downsampled by factors 2 and 4. Thus, each discriminator learns features in a different frequency range. Since the model operates at $f_s = 22.05$ kHz, D_1 observes frequency components up to the Nyquist limit $f_s/2 = 11.03$ kHz, D_2 up to $f_s/4 = 5.51$ kHz and D_3 only to $f_s/8 = 2.76$ kHz. Although our main interest is to reconstruct the frequency components above 3.0 kHz, using D_3 is still beneficial to stabilize the adversarial training and leads to better convergence. The architecture of each of the discriminators consists of a stack of grouped strided convolutions, and the down-sampling is performed by average pooling, as detailed in [48].

Time-domain discriminators are highly sensitive to phase mismatches in the data. This is a very convenient property when using a spectrogram-based generator, since maintaining the phase coherence when the audio data is transformed to the complex STFT domain may be problematic. Moreover, time-domain discriminators help keep the quasi-periodic structure of raw audio, generating a more naturally sounding harmonic series. We also experimented incorporating STFT-based discriminators, following the methodology suggested by Su *et al.* [13], but we noticed a considerable decline in the generated audio quality. The STFT discriminators force the generator to inpaint harmonic-like shapes in the spectrogram without taking into account their coherence with the lower part of the spectrum, thus generating metallic and unrealistic sounds.

In this work, we apply the least-squares GAN objective [49]. The adversarial loss for the generator is then defined as

$$L_{\text{adv}} = \mathbb{E}_{\hat{y}_k} \left[\sum_k (D_k(\hat{y}_k) - 1)^2 \right], \quad (2)$$

where \mathbb{E} is the expectation operator. The discriminators are optimized by minimizing the loss function:

$$L_{D_k} = \frac{1}{2} \mathbb{E}_{y_k} [(D_k(y_k) - 1)^2] + \frac{1}{2} \mathbb{E}_{\hat{y}_k} [D_k(\hat{y}_k)^2]. \quad (3)$$

We use the multi-resolution STFT loss [50] as the auxiliary reconstruction loss L_{rec} . This loss is defined as the expectation of the sum of two terms, $L_{\text{sc}}^{(m)}$ and $L_{\text{mag}}^{(m)}$, at M different frequency resolutions as

$$L_{\text{rec}}^{(m)} = \mathbb{E}_{y, \hat{y}} \left[\frac{1}{M} \sum_{m=1}^M L_{\text{sc}}^{(m)} + L_{\text{mag}}^{(m)} \right]. \quad (4)$$

¹https://github.com/elomoliner/bwe_historical_recordings

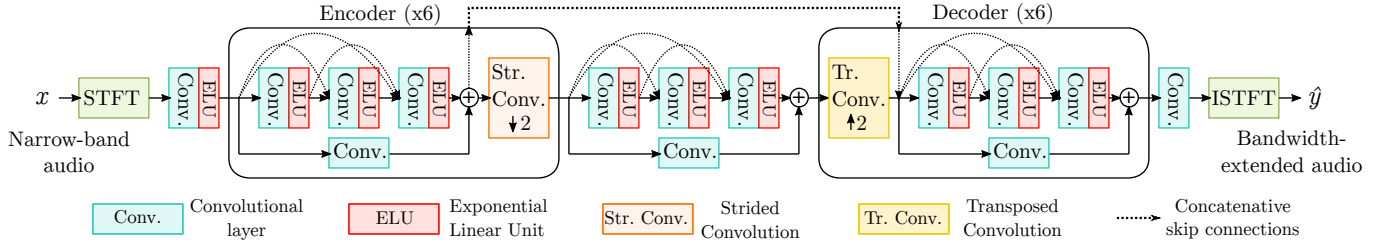


Fig. 4. Proposed U-net-based architecture of the generator model, cf. Fig. 3.

The spectral convergence term $L_{sc}^{(m)}$ and the log magnitude distance term $L_{mag}^{(m)}$ are defined, respectively, as:

$$L_{sc}^{(m)} = \frac{\| |Y^{(m)}| - |\hat{Y}^{(m)}| \|_F}{\| |Y^{(m)}| \|_F} \quad (5)$$

and

$$L_{mag}^{(m)} = \frac{1}{S} \|\log |Y^{(m)}| - \log |\hat{Y}^{(m)}|\|_1, \quad (6)$$

where $Y^{(m)}$ and $\hat{Y}^{(m)}$ are the STFTs of the signals y and \hat{y} , respectively, using an analysis window of length $m \in \{256, 512, 1024, 2048\}$, $\|\cdot\|_F$ is the Frobenius norm, $\|\cdot\|_1$ is the L1 norm, and S is the total number of STFT bins. Note that this reconstruction loss is only aware of the magnitude differences in the spectrogram, as we rely on the adversarial loss term to deal with the phase information.

C. Dataset

We train and evaluate our method using solo piano classical music. Doing so, we reduce the difficulty of the problem by limiting the variance in the training data. Piano sounds are a convenient choice for evaluating bandwidth-extension algorithms, since they contain both transient and tonal components. Moreover, since the piano is one of the most common musical instruments for solo performances, a large quantity of contemporary and historical solo piano recordings is publicly available. Considering that classical music is a genre that has practically remained unchanged over time, we avoid introducing a major divergence between the training and target distributions.

We collected our training data from the solo piano pieces of the MusicNet dataset [51], but discarded some of the older recordings as they contained heavy background noise and the audio quality was suboptimal. Overall, we use 15.5 h of broadband piano classical music for training and evaluation.

D. Lowpass Filter Generalization

Since the frequency responses in historical music recordings are far from being deterministic, we apply a lowpass filter with a randomized cutoff frequency f_c to the training data. We parameterize the cutoff frequency with a normal distribution, whose mean and standard deviation are set up empirically to be a rough estimate of the frequency responses in the gramophone recordings in the 1920s.

Based on our findings from the spectral analysis in Sec. III, we set the mean cutoff frequency to $\mu_{f_c} = 3.0$ kHz and the

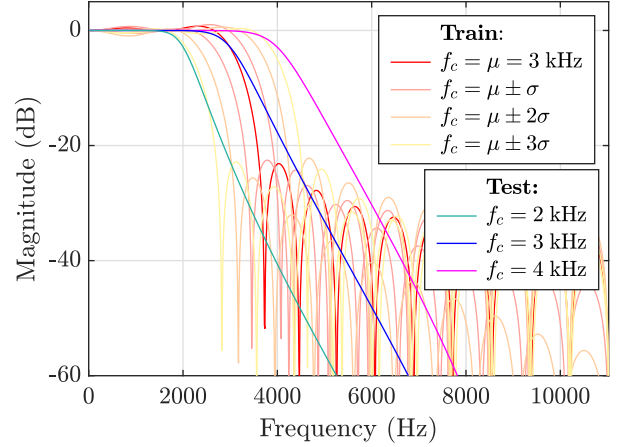


Fig. 5. Magnitude responses of lowpass filters used for training and testing.

standard deviation to $\sigma_{f_c} = 300$ Hz. The value of σ_{f_c} is the result of a trade-off off bias against variance in the model. In other words, a model trained with a larger σ_{f_c} would probably generalize to a wider range of cutoff frequencies. However, the resulting quality would likely diminish due to the increase in variance in the data, making the optimization more challenging and unstable. The lowpass filters are 25th-order FIR filters using the windowing method with the Kaiser window ($\beta = 1$). The magnitude responses of the FIR filters used for training are presented in Fig. 5. FIR filters have the convenient advantage that they can be efficiently implemented by applying convolution, thus not demanding much extra computation during training.

The idea of applying variable-band filters was also studied by Li *et al.* [14], with the difference that they used a uniform distribution instead of a normal one. Randomizing the cutoff frequency of the filter indeed helps to increase the robustness of the model in different frequency ranges, but, as we show with our experiments in Sec. V-D, randomization is certainly not enough if we want to successfully make inferences in historical recordings.

To further regularize the model, we apply a well known regularization approach [52] and corrupt the lowpass-filtered training data by adding a small amount of Gaussian white noise w having zero mean and a fixed power $\sigma^2 = -30$ dB directly to the raw audio signal. The added noise diffuses the magnitude response of the filter, as Fig. 6 demonstrates, and successfully enforces the model to generate new high-frequency content instead of overfitting the filter shape. The

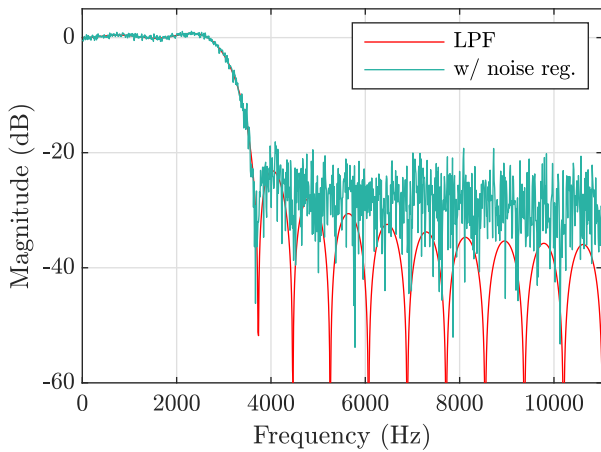


Fig. 6. Magnitude response of one of the lowpass filters used during training and its equivalent response after applying the noise regularization.

use of the additive noise during training also encourages the generator to focus only on the most prominent musical features making the model robust to the minuscule denoising residuals that it may encounter while making inferences in historical recordings. Furthermore, this noise regularization strategy injects stochasticity into the model. Given that we do not add a latent vector z to the generator, this extra noise allows the generator to produce stochastic outputs.

E. Making inferences in Historical Recordings

Using the proposed regularization, the generator can be applied to make inferences on out-of-distribution historical music recordings. Our inference pipeline builds on previous work on denoising [17], as illustrated in Fig. 1. The original noisy recordings are first denoised to suppress clicks, hisses, and other additive disturbances. Then, the denoised recordings are bandwidth-extended by directly applying the pre-trained STFT-based generator.

In the same way as during training, the noise regularization could be added at the inference stage before feeding the denoised recording to the bandwidth-extension generator. As discussed in Sec. V-B, this step helps to achieve better objective metrics. However, in the majority of the tested cases, no perceptual differences were noticed with or without noise during inference and hence it is left as an optional step.

F. Implementation Details

The used sampling frequency $f_s = 22.050$ kHz sets the upper limit of processing to about 11 kHz. This choice makes the training fast and still leaves a wide range from about 3 to 11 kHz for bandwidth extension. For training, we used batches of four audio segments, each with a duration of 5 s. Nevertheless, due to the nature of convolutional neural networks, the input length can be set arbitrarily during inference. With the goal to make the model robust to different volume (loudness) levels, we also apply a uniformly random gain, set between -6 dB and 4 dB for each input signal. We did not find using batch normalization or weight normalization beneficial to the

generator. The discriminators, however, are weight-normalized [53].

We use the Adam optimizer [54] with the parameters $\beta_1 = 0.5$ and $\beta_2 = 0.9$ to train both the generator G and the discriminators D_k . The training is divided into two separate stages. First, we train G for 10,000 steps with a learning rate of 1×10^{-4} using only the reconstruction loss L_{rec} . This step guarantees that the model learns to apply an identity mapping to the low-frequency components before including the adversarial discriminators into the training loop. Then, we decrease the learning rate to 1×10^{-5} , incorporate the adversarial loss L_{adv} , and continue training for 300,000 steps. During the second stage, the discriminators D_k are updated twice for every step taken by the generator, using a learning rate of 1×10^{-4} . The training took, on average, two days to complete on a single Tesla V100 GPU in Triton, Aalto University’s computing cluster.

V. EXPERIMENTS AND RESULTS

This section evaluates the quality of the bandwidth-extension using both objective and subjective experiments.

A. Comparison Models

We compare our proposed method with two baselines, AudioUnet [11] and SEANet [14], which were trained using the same lowpass filters and noise regularization as the BEHM-GAN. AudioUnet, a supervised model based on a time-domain U-Net [11], is trained using a reconstruction L2 loss between the resulting output waveform and the original unfiltered audio. We use the PyTorch implementation of the model released by Sulun and Davies².

SEANet is a GAN-based model that was used for speech enhancement [55] and bandwidth extension [14]. Its generator is a time-domain U-Net with dilated convolutions at the intermediate layers. An effort was made to replicate the implementation details from the larger non-real-time model evaluated in [14]. Given that the original SEANet utilizes very similar, if not the same, time-domain discriminators as in this paper, we opted to train SEANet using the same training objective as ours. This gave us better performance than the “feature” loss the authors originally applied and allowed us to directly evaluate the effects of using a complex-spectrogram generator versus a time-domain one.

We also experimented with TFiLM [33], the GAN-based HiFi-GAN [13], and the diffusion probabilistic NU-Wave models [15]. However, we did not obtain positive results using these methods for bandwidth-extending historical recordings. We hypothesize that, in contrast to speech, the aforementioned models may not be well suited for processing music instead of speech or that further hyperparameter optimization is necessary to adapt the models to our training methodology. We decided not to include these baselines in the formal evaluation to avoid reporting misleading results and to not overload the number of listening conditions in the subjective evaluation.

So as to understand the effects of the main components of our approach, we also include three ablated versions of

²<https://github.com/serkansulun/deep-music-enhancer>

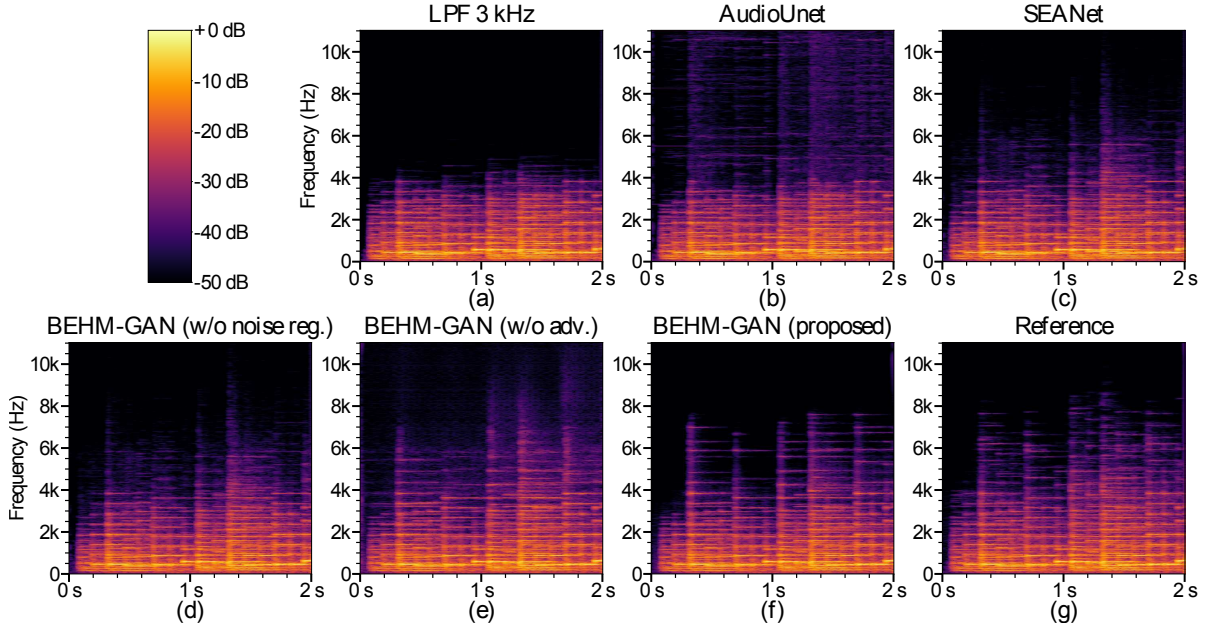


Fig. 7. Spectrograms of (a) a lowpass filtered reference signal, (b), (c), (d), (e), (f) its bandwidth-extended versions, and (g) a reference modern piano recording.

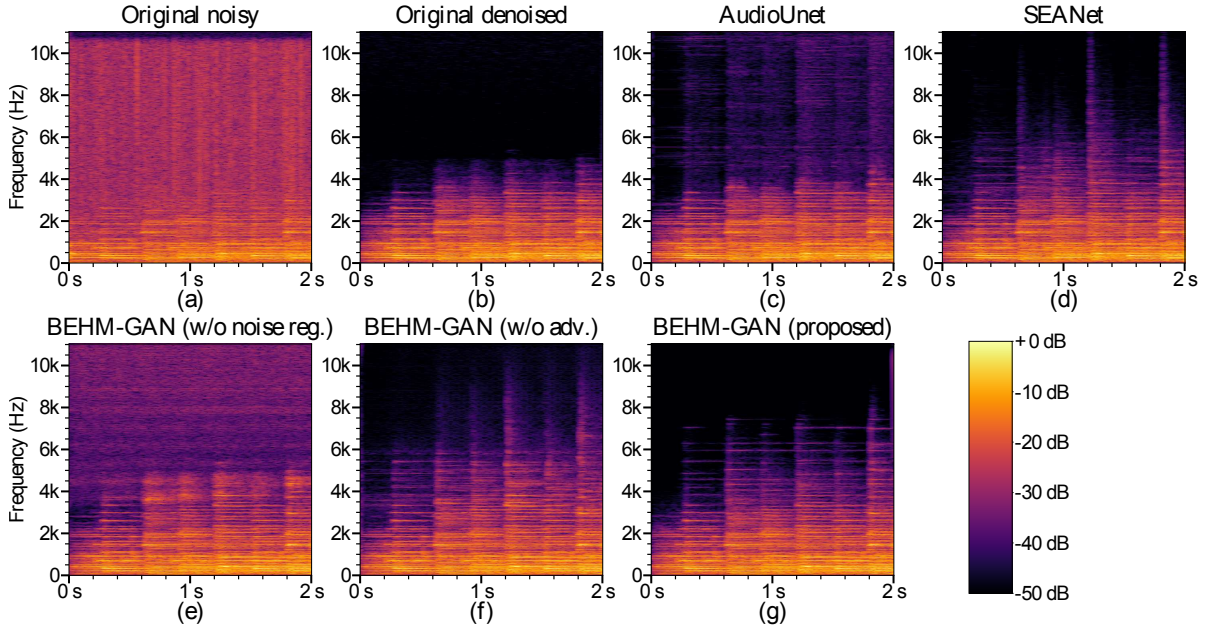


Fig. 8. Spectrograms of (a) an original noisy historical recording, (b) its a denoised version, and (c), (d), (e), (f), (g) the bandwidth-extended versions of (b).

our model in the formal evaluation. Firstly, we study the importance of noise regularization by training a model without adding white noise (w/o noise reg.). Secondly, we switch the adversarial training objective for an L2 reconstruction loss in the complex-spectrogram domain (w/o adv.). The multi-resolution STFT loss L_{rec} is not used, being ineffective if used alone, since the phase information in the spectrogram is ignored. We also report, although only with objective metrics, the effect of adding noise to the input audio signal during inference, in the same way as we do during training (with noise inf.).

Figs. 7 and 8 show a visual comparison of the spectrogram representations of the compared models in a modern-lowpass filtered example and an old recording, respectively. Figs. 7(a) and 8(b) present, respectively, the narrow-band input signals for the examples, and the other spectrograms visualize how each method recreates the missing high-frequency content. The reference signal is added in Fig. 7(g) so that the results can be compared with the original real spectrogram. As is evident, some of the compared methods produce a more realistic spectra than others. A reference signal is unavailable for the old recording in Fig. 8. In this case, we additionally present

the spectrogram of the noisy old recording before applying the denoiser in Fig. 8(a), which reveals that the old recordings contains only noise and distortion above about 4 kHz.

B. Objective Evaluation

The test set contains 70 min of modern classical piano recordings, different from the training set. All the audio signals from the test set were resampled at the rate $f_s = 22.05$ kHz and were split into non-overlapping 5-s segments. A sixth-order Butterworth lowpass filter is applied at the fixed cutoff frequency of 2 kHz, 3 kHz, and 4 kHz to imitate different bandwidth limitations. Note that the testing filters are purposely different from the training filters in order to evaluate the models in out-of-distribution filtering conditions. The magnitude responses of the three Butterworth filters used for testing are shown in Fig. 5, together with the filters used during training.

The proposed method and the aforementioned baselines are evaluated using three objective metrics: log-spectral distance (LSD), VGG distance (VGG), and Fréchet Audio Distance (FAD) [56].

1) *Log-Spectral Distance*: The LSD, a frequency-domain metric that has been popularly used in bandwidth-extension literature [11], [12], [13], [40], is defined as:

$$\text{LSD} = \frac{1}{T} \sum_{t=1}^T \sqrt{\frac{1}{K} \sum_{k=1}^K \left(\log |Y_{t,k}|^2 - \log |\hat{Y}_{t,k}|^2 \right)^2}, \quad (7)$$

where $Y_{t,k} = \text{STFT}(y)$ and $\hat{Y}_{t,k} = \text{STFT}(\hat{y})$ are the STFTs of the reference y and the bandwidth-extended audio signal \hat{y} , respectively. For the STFT computation, an analysis window of 2048 samples and a hop length of 512 samples is used.

2) *VGG Distance*: This metric is defined as the L2 distance between pairs of individual embeddings given by the VGGish network [57]. The VGGish network has been pre-trained for large-scale audio classification. Thus, this metric is expected to provide a distance measure focusing on the higher level features of the audio data. This metric was previously used to evaluate music denoising [4] and bandwidth-extension [16] methods.

3) *Fréchet Audio Distance*: FAD [56] has been adapted for audio from the Fréchet Inception Distance (FID), a frequently used metric to evaluate image-generative models. This metric also uses the VGGish embeddings to compare the statistics between two collections of audio. FAD fits a multivariate normal distribution to a collection of background $\mathcal{N}(\mu_b, \Sigma_b)$ and evaluation $\mathcal{N}(\mu_e, \Sigma_e)$ embeddings. Then, the Fréchet distance between both distributions is defined as:

$$\text{FAD} = \|\mu_b - \mu_e\|_2 + \text{tr}(\Sigma_b + \Sigma_e - 2\sqrt{\Sigma_b \Sigma_e}), \quad (8)$$

where $\|\cdot\|_2$ is the L2 norm and $\text{tr}(\cdot)$ is the trace of a matrix. Being reference-free, we avoid computing FAD on paired data by dividing the test set into two equally-sized splits. One of them is used to compute the background statistics, whereas the second is used to evaluate the different models.

The FAD can also be used to evaluate the bandwidth-extension performance in real historical recordings. Similarly, the FAD is computed from 15 min of historical recordings

using the same background statistics. The six historical recordings that we use for evaluation were extracted from “The Great 78 Project” [58], a large collection of publicly available digitized 78-RPM gramophone records [59]. However since the FAD has the limitation of working at the sampling frequency of 16 kHz, which differs from that at which the BEHM-GAN operates (22.05 kHz), the audio signals must be resampled before computing this metric. As a consequence, the FAD only observes frequency components up to the Nyquist limit of 8 kHz, missing some high-frequency details. The study of the design of broadband reference-free audio quality metrics is left as future work.

No SNR-related metric is used for the objective evaluation because they are extremely sensitive to phase misalignments between pairs of data. Since the training and testing filters have a different phase response, the waveform representations of the reference and the bandwidth-extended audio can differ greatly, although they may sound similar. For this reason, the SNR results do not correlate with perceptual audio quality and are discarded.

The objective results are tabulated in Table I. Note that a reference condition for the FAD metrics is added in the lowpass filtered results. This refers to computing the FAD between the two test splits of broadband piano recordings. Thus, the reference results can be considered as a lower bound of the FAD metric.

The proposed method outperforms the two compared baselines in all the evaluated conditions and, most importantly, improves over the “LPF/Original” condition, where no bandwidth extension was applied. The performance decreases when the noise regularization is not used, and also when the model is trained without the adversarial losses, which seems to prove the point that these are critical features of the model. We will return to this point when analyzing the subjective evaluation results in Sec. V-D.

The BEHM-GAN obtains the most substantial improvement when $f_c = 3$ kHz, which corresponds to the mean cutoff frequency used for the training filters. The model also generalizes well when the cutoff frequency is higher ($f_c = 4$ kHz). However, when decreasing the cutoff frequency ($f_c = 2$ kHz), the metrics deteriorate a little as the task gets considerably harder. Nevertheless, even in this case, a significant improvement is seen in all three metrics with respect to the unprocessed lowpass filtered condition. The objective metrics also show that the FAD is decreased by a factor of two when the BEHM-GAN is evaluated with real historical recordings, implying that the model is able to generalize in this real-world case.

The metrics of the proposed method consistently improve when noise regularization is added at the inference stage. This is an expected result given that, in this case, the test example gets closer to the training distribution. However, as seen in Table II, this does not necessarily happen with the other baseline methods. We noticed that AudioUnet and, to a lesser extent, SEANet sometimes do not succeed at completely suppressing the extra added Gaussian noise. No perceptual improvement was observed in the BEHM-GAN with or without noise added during inference or not. As a consequence, to make a fair comparison, only versions with

TABLE I
OBJECTIVE METRICS, WHERE LOWER IS BETTER FOR ALL CASES. THE BEST RESULT IN EACH COLUMN IS HIGHLIGHTED

	$f_c = 2$ kHz			$f_c = 3$ kHz			$f_c = 4$ kHz			Historical recording
	LSD	VGGish	FAD	LSD	VGGish	FAD	LSD	VGGish	FAD	
LPF/Original	1.01	5.38	4.96	0.82	3.93	3.48	0.71	3.43	2.07	2.16
AudioUnet	0.99	4.57	3.51	0.84	3.99	1.96	0.79	3.73	1.56	2.88
SEANet	0.99	4.41	3.87	0.81	3.38	1.18	0.75	3.21	1.05	1.66
BEHM-GAN (proposed)	0.87	4.15	3.44	0.71	3.21	0.70	0.66	3.01	0.70	1.26
w/o noise reg.	0.92	4.45	5.14	0.73	3.54	2.60	0.7	3.47	1.04	6.00
w/o adv.	1.00	5.42	5.18	0.86	3.99	2.95	0.75	4.02	1.91	2.23
with noise inf.	0.85	3.98	3.34	0.71	3.00	0.68	0.66	2.76	0.64	1.12
Reference	-	-	0.58	-	-	0.58	-	-	0.58	-

TABLE II
COMPARISON STUDY OF ADDING NOISE AT THE INFERENCE STAGE. THE BEST RESULT IN EACH ROW IS HIGHLIGHTED

		FAD	
		w/o noise at inf.	with noise at inf.
Lowpass filtered $f_c = 3$ kHz	AudioUnet	1.96	3.64
	SEANet	1.18	1.09
	BEHM-GAN	0.70	0.68
Historical recordings	AudioUnet	2.88	6.74
	SEANet	1.66	1.91
	BEHM-GAN	1.26	1.12

no extra noise are included in the subjective evaluations.

C. Subjective Evaluation of Synthetic Filtered Data

Since finding an objective metric that correlates with human perception is not easy, a formal subjective evaluation is conducted. We designed a blind listening test structured as two consecutive sessions, one to assess the performance of our method with simulated lowpass filtered piano music and the other to evaluate the performance in real historical piano recordings, which is detailed in Sec. V-D.

The first part was designed following the MUSHRA recommendation [60] with the purpose to evaluate the bandwidth-extension performance in synthetic lowpass filtered recordings. The listeners had to grade, on a perceptual scale from 0 to 100, the audio quality in eight different conditions. The reference signal was a contemporary broadband recording, expected to be rated as 100. Another condition was a lowpass filtered version of the reference at the cutoff frequency of 3 kHz (LPF 3kHz), applying the same Butterworth filter that was used in the objective evaluation. The rest of the conditions were five different bandwidth-extended versions of the lowpass filtered signal, using the same methods as in Sec. V-B. Also included as a low anchor is an easy-to-recognize poor-quality signal lowpass filtered at 1.5 kHz, which was expected to be graded as 0 by the listeners. We included six different 10-s piano music examples, repeated twice in random order, forming a total of 12 pages in the MUSHRA test. The audio examples included in the test are available listen at the companion webpage³.

Altogether, 13 listeners participated in the listening test. However, one participant was discarded from the first part

because they did not identify the reference in more than 15% of the occasions, as recommended in [60]. All subjects had previous experience in formal listening tests, three of them were female, and their average age was 29 years. The two test sessions took, on average, 45 min to complete. The experiment was conducted in the sound-proof listening booths of the Aalto Acoustics Lab, providing the same isolated listening conditions for all subjects. The listening test was implemented using the webMUSHRA interface [61] that allowed the listeners to set loops if they wanted to focus on particular short passages of the audio signal. This feature was particularly useful for some participants, since the most noticeable differences between the conditions were localized in certain details, such as at the attack transients of the piano tones.

The results of the first session are plotted in Fig. 9. Table III presents the distances between the median scores of the BEHM-GAN and the compared conditions. The level of statistical significance given by a paired t-test is also marked. Examples 3, 4, and 6 contained intense *fortissimo* piano passages, where the effect of the bandwidth limitation was easily audible. This explains why all the compared models obtained consistently lower ratings in these examples than in Examples 1, 2, and 5, which were softer and contained less high-frequency content.

For all six examples, the proposed method obtained higher median scores than the other evaluated conditions. As indicated in paired t-tests (see Table III), most differences are statistically significant. The subjects easily identified the reference in all the examples except examples 2 and 5, where a large proportion of listeners rated the BEHM-GAN with the maximum score of 100.

The worst-rated model was AudioUnet, which introduced some annoying aliasing artifacts that can be seen at the upper part of Fig. 7(b). SEANet worked significantly better but still produced a slightly distorted sound. The ablated versions of the proposed method obtained relatively good scores but, in the majority of the cases, were outperformed by the full BEHM-GAN model.

D. Subjective Evaluation of Historical Recordings

The goal of the second session of the listening test was to evaluate the performance of the compared models in real historical recordings. The test method was a modified version of MUSHRA [60], where the audio examples were historical

³<http://research.spa.aalto.fi/publications/papers/ieee-taslp-behm-gan/>

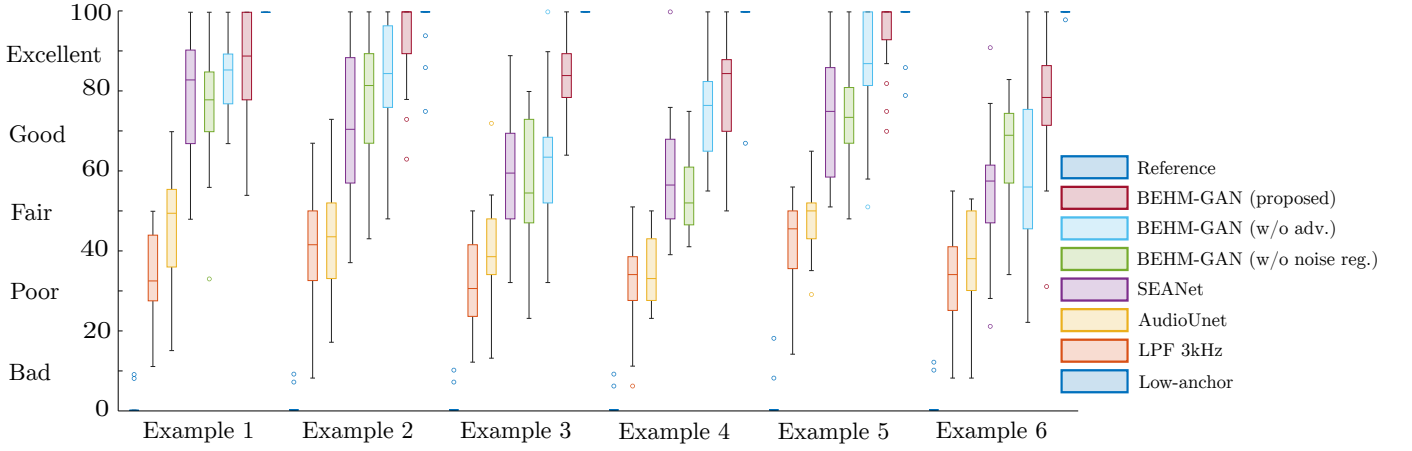


Fig. 9. Box-plot visualizations of the listening test results on synthetic lowpass filtered recordings.

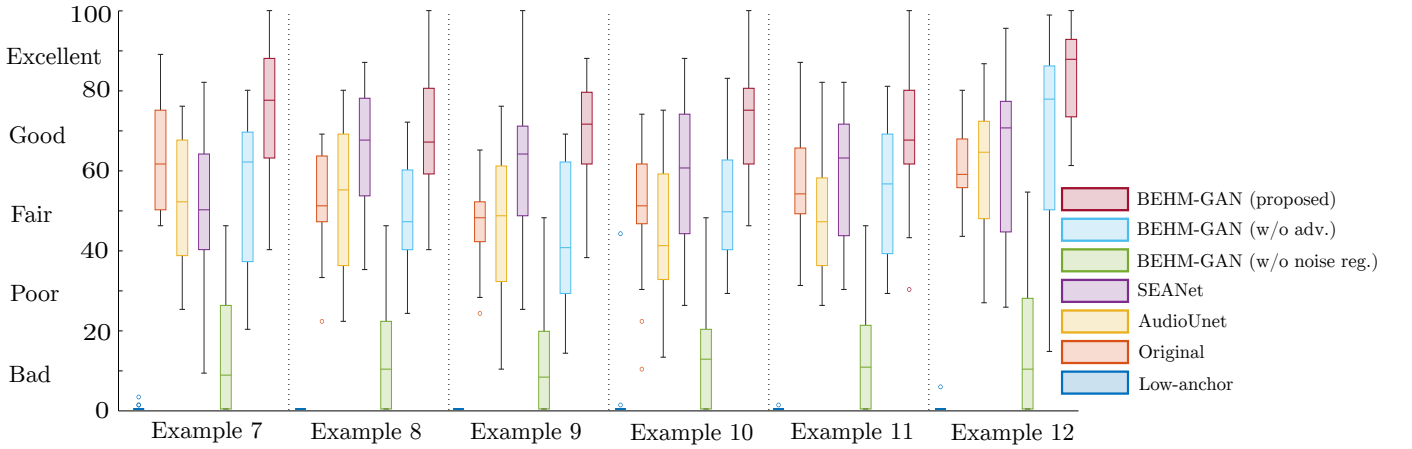


Fig. 10. Box-plot visualizations of the listening test results on real historical recordings.

piano recordings. Since a broadband reference is unavailable, the reference presented to the listeners was a denoised narrow-band gramophone recording. The tested conditions were the various bandwidth-extended versions of the reference, using the same methods as in the previous session. The same low anchor was included with the expectation of it being graded as 0, forming a total of seven conditions. The participants were asked to grade the audio quality for each of the conditions on a scale from 0 to 100 with the same criteria as in the first session, where 100 corresponds to a hypothetical perfect version of the reference. Thus, the participants were discouraged to rate any of the conditions with a score of 100 unless the quality was considered enhanced in a perfectly realistic manner. The second session included six 10-s examples of historical piano recordings, also repeated twice, and the total number of MUSHRA pages was 12.

The experiment was conducted consecutively after the first session in the same conditions, with a short break between the two sessions. The test participants were also the same, except one who had to be discarded from the second part as they misunderstood the test question. This session took, on average, 20 min to complete.

The results of the second session are presented in Fig. 10 and Table IV. Given that a higher “excellent” anchor was not

available, the resulting scores contain more variance. Every participant had a slightly different idea of how an excellent-quality piano recording should sound. This explains the wider confidence intervals. Nevertheless, valuable conclusions can be extracted on how well each model generalizes to real historical recordings.

The BEHM-GAN obtained significantly better results than the original recording in all the examples, implying that the bandwidth extension improved the sound quality. The other compared models introduced some distortion artifacts that the listeners sometimes evaluated negatively. The proposed method obtained marginally better scores than the rest of the conditions in all the examples except example 8, where SEANet received a slightly higher median score. Nevertheless, the BEHM-GAN outperformed SEANet in four out of six examples, as is evident from Table IV. After finishing the test, some participants commented that the enhancement was often more noticeable with the time-domain SEANet model. However, the proposed method produced more realistic results, despite being more conservative.

Both ablated conditions suffered from a decline in performance. In particular, when noise regularization was ablated (BEHM-GAN w/o noise reg.), the resulting metrics were disappointing. These results can be explained by looking at

the example in Fig. 8(e), which looks noisy and distorted. We hypothesize that the model learned to invert the frequency response of a hypothetical lowpass filter but it failed when it encountered an out-of-distribution example where no such filter was applied. By closely inspecting the spectrogram of Fig. 8(e), the model is observed to significantly boost the frequency bands above 4 kHz and introduce some horizontally-shaped noisy components that resemble the side lobes of the lowpass filters seen during training. These results show that noise regularization is critical for the good performance of our system. Another observation is that the non-adversarial condition (BEHM-GAN w/o adv.) obtained worse scores in this case, implying that the proposed adversarial training objective is highly beneficial to generate a more realistic enhancement in this out-of-distribution scenario.

VI. CONCLUSIONS

This paper proposes the BEHM-GAN, a method to extend the bandwidth of historical music. The proposed method is based on a generative adversarial network and combines a complex-spectrogram-domain generator with multiple time-domain discriminators. The BEHM-GAN is trained in a self-supervised fashion using lowpass filters to simulate the bandwidth limitation of old recordings. With the intention of strengthening the robustness of our model, we regularize the training by randomizing the cutoff frequency of the filters and perturbing the filtered signal with a small amount of Gaussian white noise. The trained generator is designed to be incorporated as the second step in a music restoration pipeline, where the first step is a deep music denoiser [17].

The proposed method is evaluated using lowpass filtered and historical piano music with objective and subjective metrics. The BEHM-GAN outperforms the two compared baselines, both of which were trained using the same proposed regularization. Additionally, ablation experiments were conducted to demonstrate the importance of the proposed adversarial training and regularization schemes to achieve good performance making inferences in real-world historical recordings. The results of a formal blind listening test show that the BEHM-GAN introduces significant quality improvement to old piano recordings. This is, to the best of our knowledge, the first successful work that extends the bandwidth of historical music recordings. Future work includes extending this work to recordings made with other musical instruments other than the piano.

APPENDIX

Tables III and IV show for each of the listening test sessions, the differences between the median scores of the proposed BEHM-GAN model and the rest of the conditions, respectively. Thus, larger positive values represent worst median scores, relative to the scores received by the proposed method. Asterisks (*) denote significant differences in a paired t-test, where *, ** and *** respectively indicate p-values < 0.05 , < 0.01 and < 0.001 .

ACKNOWLEDGMENT

The authors would like to thank the participants of the listening test. Special thanks go to Mr. Luis Costa for proof-reading the manuscript. Additionally, the authors acknowledge the computational resources provided by the Aalto Science-IT project.

REFERENCES

- [1] S. J. Godsill and P. J. W. Rayner, *Digital Audio Restoration—A Statistical Model Based Approach*. Springer, 1998.
- [2] P. A. A. Esquef, “Audio restoration,” in *Handbook of Signal Processing in Acoustics*. New York, NY, USA: Springer, 2008, pp. 773–784.
- [3] F. Rund, V. Vencovský, and M. Semanský, “An evaluation of click detection algorithms against the results of listening tests,” *J. Audio Eng. Soc.*, vol. 69, no. 7/8, pp. 586–593, July/Aug. 2021.
- [4] Y. Li, B. Gfeller, M. Tagliasacchi, and D. Roblek, “Learning to denoise historical music,” in *Proc. 21st ISMIR Conf.*, Montréal, Canada, Oct. 2020, pp. 504–511.
- [5] N. Perraudin, N. Holighaus, P. Majdak, and P. Balazs, “Inpainting of long audio segments with similarity graphs,” *IEEE/ACM Trans. Audio Speech Lang. Process.*, vol. 26, no. 6, pp. 1083–1094, Jun. 2018.
- [6] A. Marafioti, P. Majdak, N. Holighaus, and N. Perraudin, “GACELA—A generative adversarial context encoder for long audio inpainting,” *IEEE J. Sel. Top. Signal Process.*, vol. 15, no. 1, pp. 120–131, Jan. 2021.
- [7] P. Závřiska, P. Rajmic, A. Ozerov, and L. Rencker, “A survey and an extensive evaluation of popular audio declipping methods,” *IEEE J. Sel. Topics Signal Process.*, vol. 15, no. 1, pp. 5–24, Jan. 2021.
- [8] M. Miron and M. Davies, “High frequency magnitude spectrogram reconstruction for music mixtures using convolutional autoencoders,” in *Proc. Int. Conf. Digit. Audio Effects*, Aveiro, Portugal, Sep. 2018, pp. 173–180.
- [9] M. Lagrange and F. Gontier, “Bandwidth extension of musical audio signals with no side information using dilated convolutional neural networks,” in *Proc. IEEE Int. Conf. Acoust. Speech Signal Process. (ICASSP)*, Barcelona, Spain, May 2020, pp. 801–805.
- [10] S. Hu, B. Zhang, B. Liang, E. Zhao, and S. Lui, “Phase-aware music super-resolution using generative adversarial networks,” in *Proc. Interspeech*, Shanghai, China, Oct. 2020.
- [11] V. Kuleshov, S. Z. Enam, and S. Ermon, “Audio super resolution using neural nets,” in *Proc. Int. Conf. Learn. Represent. (ICLR) (Workshop Track)*, Toulon, France, Apr. 2017.
- [12] H. Wang and D. Wang, “Towards robust speech super-resolution,” *IEEE/ACM Trans. Audio Speech Lang. Process.*, vol. 29, pp. 2058–2066, Jan. 2021.
- [13] J. Su, Y. Wang, A. Finkelstein, and Z. Jin, “Bandwidth extension is all you need,” in *Proc. IEEE Int. Conf. Acoust. Speech Signal Process. (ICASSP)*, Toronto, Canada, Jun. 2021, pp. 696–700.
- [14] Y. Li, M. Tagliasacchi, O. Rybakov, V. Ungureanu, and D. Roblek, “Real-Time Speech Frequency Bandwidth Extension,” in *Proc. IEEE Int. Conf. Acoust. Speech Signal Process. (ICASSP)*, Toronto, Canada, Jun. 2021, pp. 691–695.
- [15] J. Lee and S. Han, “NU-Wave: A diffusion probabilistic model for neural audio upsampling,” in *Proc. Interspeech*, Brno, Czech Republic, Aug. 2021, pp. 1634–1638.
- [16] S. Sulun and M. E. Davies, “On filter generalization for music bandwidth extension using deep neural networks,” *IEEE J. Sel. Top. Signal Process.*, vol. 15, no. 1, pp. 132–142, Nov. 2020.
- [17] E. Moliner and V. Välimäki, “A two-stage U-Net for high-fidelity denoising of historical recordings,” in *Proc. IEEE Int. Conf. Acoust. Speech Signal Process. (ICASSP)*, Singapore, May 2022, accepted for publication.
- [18] I. Goodfellow, J. Pouget-Abadie, M. Mirza, B. Xu, D. Warde-Farley, S. Ozair, A. Courville, and Y. Bengio, “Generative adversarial nets,” in *Proc. Adv. Neural Inf. Process. Syst. (NeurIPS)*, Montreal, Canada, Dec. 2014.
- [19] E. Larsen and R. Aarts, *Audio Bandwidth Extension: Application of Psychoacoustics, Signal Processing and Loudspeaker Design*. Wiley, 2005.
- [20] M. Nilsson and W. B. Kleijn, “Avoiding over-estimation in bandwidth extension of telephony speech,” in *Proc. IEEE Int. Conf. Acoust. Speech Signal Process. (ICASSP)*, Salt Lake City, UT, USA, 2001, pp. 869–872.
- [21] T. Ziegler, A. Ehret, P. Ekstrand, and M. Lutzky, “Enhancing MP3 with SBR: Features and capabilities of the new mp3PRO algorithm,” in *Proc. Audio Eng. Soc. 112th Conv.*, Munich, Germany, Apr. 2002.

TABLE III
DIFFERENCES BETWEEN THE MEDIAN SCORES OF THE LISTENING TEST ON SYNTHETIC FILTERED RECORDINGS

	Synthetic Lowpassed Recordings					
	Ex. 1	Ex. 2	Ex. 3	Ex. 4	Ex. 5	Ex. 6
Low-anchor	89 ***	100 ***	84 ***	84.5 ***	100 ***	78.5 ***
LPF 3kHz	56.5 ***	58.5 ***	53.5 ***	50.5 ***	54.5 ***	44.5 ***
AudioUnet	39.5 ***	56.5 ***	45.5 ***	51.5 ***	50 ***	40.5 ***
SEANet	6	29.5 ***	24.5 ***	28 ***	25 ***	21 ***
BEHM-GAN (w/o noise reg.)	11 *	18.5 **	29.5 ***	32.5 ***	26.5 ***	9.5 **
BEHM-GAN (w/o adv.)	3.5	15.5 *	20.5 ***	8	13 *	22.5 ***
Reference	-15 ***	0	-16 ***	-15.5 ***	0	-21.5 ***

TABLE IV
DIFFERENCES BETWEEN THE MEDIAN SCORES OF THE LISTENING TEST ON REAL HISTORICAL RECORDINGS

	Real Historical Recordings					
	Ex. 7	Ex. 8	Ex. 9	Ex. 10	Ex. 11	Ex. 12
Low-anchor	77.5 ***	67 ***	71.5 ***	75 ***	67.5 ***	79 ***
Original (denoised)	16 *	16 ***	23.5 ***	24 ***	13.5 *	26 ***
AudioUnet	25.5 ***	12 **	23 ***	34 ***	20.5 ***	21 ***
SEANet	27.5 ***	-0.5	7.5	14.5 **	4.5 *	15.5 ***
BEHM-GAN (w/o noise reg.)	69 ***	57 ***	63.5 ***	62.5 ***	57 ***	70 ***
BEHM-GAN (w/o adv.)	15.5 ***	20 ***	31 ***	25.5 ***	11 **	9 *

- [22] Q. Huang, T. Liu, X. Wu, and T. Qu, "A generative adversarial net-based bandwidth extension method for audio compression," *J. Audio Eng. Soc.*, vol. 67, no. 12, pp. 986–993, Dec. 2019.
- [23] J. Makhoul and M. Berouti, "High-frequency regeneration in speech coding systems," in *Proc. IEEE Int. Conf. Acoust. Speech Signal Process. (ICASSP)*, Washington D.C., USA, Apr. 1979, pp. 428–431.
- [24] M. Dietz, L. Liljeryd, K. Kjørling, and O. Kunz, "Spectral band replication, a novel approach in audio coding," in *Proc. Audio Eng. Soc. 112th Conv.*, Munich, Germany, Apr. 2002.
- [25] K.-Y. Park and H. S. Kim, "Narrowband to wideband conversion of speech using GMM based transformation," in *Proc. IEEE Int. Conf. Acoust. Speech Signal Process. (ICASSP)*, Istanbul, Turkey, Jun. 2000, pp. 1843–1846.
- [26] H. Seo, H.-G. Kang, and F. Soong, "A maximum a posteriori-based reconstruction approach to speech bandwidth expansion in noise," in *Proc. IEEE Int. Conf. Acoust. Speech Signal Process. (ICASSP)*, Florence, Italy, May. 2014, pp. 6087–6091.
- [27] P. Jax and P. Vary, "Artificial bandwidth extension of speech signals using MMSE estimation based on a hidden Markov model," in *Proc. IEEE Int. Conf. Acoust. Speech Signal Process. (ICASSP)*, Hong Kong, China, Apr. 2003, pp. 680–683.
- [28] J. Kontio, L. Laaksonen, and P. Alku, "Neural network-based artificial bandwidth expansion of speech," *IEEE Trans. Audio Speech Lang. Process.*, vol. 15, no. 3, pp. 873–881, Feb. 2007.
- [29] H. Pulakka and P. Alku, "Bandwidth extension of telephone speech using a neural network and a filter bank implementation for highband mel spectrum," *IEEE Trans. Audio Speech Lang. Process.*, vol. 19, no. 7, pp. 2170–2183, Aug. 2011.
- [30] K. Li and C.-H. Lee, "A deep neural network approach to speech bandwidth expansion," in *Proc. IEEE Int. Conf. Acoust. Speech Signal Process. (ICASSP)*, South Brisbane, QLD, Australia, Apr. 2015, pp. 4395–4399.
- [31] K. Li, Z. Huang, Y. Xu, and C. Lee, "DNN-based speech bandwidth expansion and its application to adding high-frequency missing features for automatic speech recognition of narrowband speech," in *Proc. Interspeech*, Dresden, Germany, Sep. 2015, pp. 2578–2582.
- [32] A. Gupta, B. Shillingford, Y. Assael, and T. C. Walters, "Speech bandwidth extension with wavenet," in *Proc. IEEE Work. App. Signal Process. Audio Acoust. (WASPAA)*, New Paltz, NY, USA, Oct. 2019, pp. 205–208.
- [33] S. Birnbaum, V. Kuleshov, Z. Enam, P. W. Koh, and S. Ermon, "Temporal FiLM: Capturing long-range sequence dependencies with feature-wise modulations," in *Proc. Adv. Neural Inf. Process. Syst. (NeurIPS)*, Virtual event, Sep. 2021.
- [34] T. Y. Lim, R. A. Yeh, Y. Xu, M. N. Do, and M. Hasegawa-Johnson, "Time-frequency networks for audio super-resolution," in *Proc. IEEE Int. Conf. Acoust. Speech Signal Process. (ICASSP)*, Calgary, Canada, Apr. 2018, pp. 646–650.
- [35] J. Lin, Y. Wang, K. Kalgaonkar, G. Keren, D. Zhang, and C. Fuegen, "A two-stage approach to speech bandwidth extension," in *Proc. Interspeech*, Brno, Czech Republic, Aug. 2021, pp. 1689–1693.
- [36] K. Zhang, Y. Ren, C. Xu, and Z. Zhao, "WSRGlow: A Glow-based waveform generative model for audio, super-resolution," in *Proc. Interspeech*, Shanghai, China, Aug. 2021, pp. 1649–1653.
- [37] M. Mirza and S. Osindero, "Conditional generative adversarial nets," Nov. 2014, arXiv:1411.1784.
- [38] P. Isola, J.-Y. Zhu, T. Zhou, and A. A. Efros, "Image-to-image translation with conditional adversarial networks," in *Proc. IEEE Comput. Soc. Conf. Comput. Vis. Pattern Recognit. (CVPR)*, Honolulu, HI, USA, Jul. 2017, pp. 1125–1134.
- [39] S. Kim and V. Sathe, "Bandwidth extension on raw audio via generative adversarial networks," Mar. 2019, arXiv:1903.09027.
- [40] S. E. Eskimez, K. Koishida, and Z. Duan, "Adversarial training for speech super-resolution," *IEEE J. Sel. Topics Signal Process.*, vol. 13, no. 2, pp. 347–358, Apr. 2019.
- [41] R. Geirhos, J.-H. Jacobsen, C. Michaelis, R. Zemel, W. Brendel, M. Bethge, and F. A. Wichmann, "Shortcut learning in deep neural networks," *Nat. Mach. Intell.*, vol. 2, no. 11, pp. 665–673, Nov. 2020.
- [42] V.-A. Nguyen, A. H. Nguyen, and A. W. Khong, "Tunet: A block-online bandwidth extension model based on transformers and self-supervised pretraining," Jan. 2022, arXiv:2110.13492.
- [43] P. Copeland, *Manual of Analogue Sound Restoration Techniques*. British Library London, UK, 2008.
- [44] C. Hummersone, "IoSR Matlab toolbox," <https://github.com/iosr-surrey/matlabtoolbox>, 2017.
- [45] D.-A. Clevert, T. Unterthiner, and S. Hochreiter, "Fast and accurate deep network learning by exponential linear units (ELUs)," in *Proc. Int. Conf. Learn. Represent. (ICLR)*, Feb. 2016. [Online]. Available: <http://arxiv.org/abs/1511.07289>
- [46] U. Isik, R. Giri, N. Phansalkar, J.-M. Valin, K. Helwani, and A. Krishnaswamy, "PoCoNet: Better speech enhancement with frequency-positional embeddings, semi-supervised conversational data, and biased loss," in *Proc. Interspeech*, Shanghai, China, Oct. 2020, pp. 2487–2491.
- [47] G. Huang, Z. Liu, L. van der Maaten, and K. Q. Weinberger, "Densely connected convolutional networks," in *Proc. CVPR*, Honolulu, HI, Jul. 2017, pp. 4700–4708.
- [48] K. Kumar, R. Kumar, T. de Boissiere, L. Gestein, W. Z. Teoh, J. Sotelo, A. de Brébisson, Y. Bengio, and A. C. Courville, "MelGAN: Generative adversarial networks for conditional waveform synthesis," in *Proc. Adv. Neural Inf. Process. Syst. (NeurIPS)*, Vancouver, Canada, Dec. 2019.
- [49] X. Mao, Q. Li, H. Xie, R. Y. Lau, Z. Wang, and S. Paul Smolley, "Least squares generative adversarial networks," in *Proc. IEEE Int. Conf. Comput. (ICCV)*, Venice, Italy, Oct. 2017, pp. 2794–2802.

- [50] R. Yamamoto, E. Song, and J.-M. Kim, "Parallel WaveGAN: A fast waveform generation model based on generative adversarial networks with multi-resolution spectrogram," in *Proc. IEEE Int. Conf. Acoust. Speech Signal Process. (ICASSP)*, Barcelona, Spain, May. 2020, pp. 6199–6203.
- [51] J. Thickstun, Z. Harchaoui, and S. M. Kakade, "Learning features of music from scratch," in *Proc. Int. Conf. Learn. Represent. (ICLR)*, Toulon, France, Apr. 2017.
- [52] C. M. Bishop, "Training with noise is equivalent to Tikhonov regularization," *Neural Comput.*, vol. 7, no. 1, pp. 108–116, 1995.
- [53] T. Salimans and D. P. Kingma, "Weight normalization: A simple reparameterization to accelerate training of deep neural networks," *Proc. Adv. Neural Inf. Process. Syst. (NeurIPS)*, vol. 29, pp. 901–909, 2016.
- [54] D. P. Kingma and J. Ba, "Adam: A method for stochastic optimization," in *Proc. Int. Conf. Learn. Represent. (ICLR)*, San Diego, CA, May 2015.
- [55] M. Tagliasacchi, Y. Li, K. Misiunas, and D. Roblek, "Seanet: A multi-modal speech enhancement network," in *Proc. Interspeech*, Shanghai, China, Oct. 2020, pp. 1126–1130.
- [56] K. Kilgour, M. Zuluaga, D. Roblek, and M. Sharifi, "Fr chet audio distance: A reference-free metric for evaluating music enhancement algorithms," in *Proc. Interspeech*, Graz, Austria, Sep. 2019, pp. 2350–2354.
- [57] S. Hershey, S. Chaudhuri, D. P. Ellis, J. F. Gemmeke, A. Jansen, R. C. Moore, M. Plakal, D. Platt, R. A. Saurous, B. Seybold *et al.*, "CNN architectures for large-scale audio classification," in *Proc. IEEE Int. Conf. Acoust. Speech Signal Process. (ICASSP)*, New Orleans, LA, USA, Mar. 2017, pp. 131–135.
- [58] "The Great 78 Project," <https://great78.archive.org>, accessed: April 14, 2022.
- [59] "The Internet Archive," <https://archive.org>, accessed: April 14, 2022.
- [60] "Method for the subjective assessment of intermediate quality level of audio systems," International Telecommunication Union, Geneva, Switzerland, Rec. BS.1534-3, Oct. 2015.
- [61] M. Schoeffler, S. Bartoschek, F.-R. St ter, M. Roess, S. Westphal, B. Edler, and J. Herre, "WebMUSHRA—A comprehensive framework for web-based listening tests," *J. Open Res. Softw.*, vol. 6, no. 1, pp. 1–8, Feb. 2018.



Vesa V lim ki (Fellow, IEEE) received his M.Sc. and D.Sc. degrees in electrical engineering from the Helsinki University of Technology (TKK), Espoo, Finland, in 1992 and 1995, respectively.

He was a Postdoctoral Research Fellow at the University of Westminster, London, UK, in 1996. In 1997–2001, he was a Senior Assistant (cf. Assistant Professor) at TKK. In 2001–2002, he was a Professor of signal processing at the Pori unit of the Tampere University of Technology. In 2008–2009, he was a Visiting Scholar at Stanford University. He

is currently a Full Professor of audio signal processing and the Vice Dean for Research in electrical engineering at Aalto University, Espoo, Finland. His research interests are in audio and musical applications of signal processing and machine learning.

Prof. V lim ki is a Fellow of the IEEE and a Fellow of the Audio Engineering Society. In 2007–2013, he was a Member of the Audio and Acoustic Signal Processing Technical Committee of the IEEE Signal Processing Society and is currently an Associate Member. In 2005–2009, he served as an Associate Editor of the IEEE SIGNAL PROCESSING LETTERS and in 2007–2011, as an Associate Editor of the IEEE TRANSACTIONS ON AUDIO, SPEECH AND LANGUAGE PROCESSING. In 2015–2020, he was a Senior Area Editor of the IEEE/ACM TRANSACTIONS ON AUDIO, SPEECH AND LANGUAGE PROCESSING. In 2007, 2015, and 2019, he was a Guest Editor of special issues of the *IEEE Signal Processing Magazine*, and in 2010, of a special issue of the IEEE TRANSACTIONS ON AUDIO, SPEECH AND LANGUAGE PROCESSING. Currently, he is the Editor-in-Chief of the *Journal of the Audio Engineering Society*.



Eloi Moliner received his B.Sc. degree in Telecommunications Technologies and Services Engineering from the Polytechnic University of Catalonia, Spain, in 2018 and his M.Sc. degree in Telecommunications Engineering from the same university in 2021.

He is currently a doctoral candidate in the Acoustics Lab of Aalto University in Espoo, Finland. His research interests include digital audio restoration and audio applications of machine learning.